

The effect of materials' rheology on process energy consumption and melt thermal quality in polymer extrusion

Chamil Abeykoon¹  | Paula Pérez¹ | Adrian L. Kelly²

¹Northwest Composites Centre, Department of Materials, Faculty of Science and Engineering, The University of Manchester, Manchester, UK

²Polymer IRC, School of Engineering and Informatics, University of Bradford, Bradford, UK

Correspondence

Chamil Abeykoon, Northwest Composites Centre, Department of Materials, Faculty of Science and Engineering, The University of Manchester, Oxford Road, Manchester M13 9PL, UK.
Email: chamil.abeykoon@manchester.ac.uk; yabeykoon01@qub.ac.uk

Abstract

Polymer extrusion is an important but an energy intensive method of processing polymeric materials. The rapid increase in demand of polymeric products has forced manufactures to rethink their processing efficiencies to manufacture good quality products with low-unit-cost. Here, analyzing the operational conditions has become a key strategy to achieve both energy and thermal efficiencies simultaneously. This study aims to explore the effects of polymers' rheology on the energy consumption and melt thermal quality (ie, a thermally homogeneous melt flow in both radial and axial directions) of extruders. Six commodity grades of polymers (LDPE, LLDPE, PP, PET, PS, and PMMA) were processed at different conditions in two types of continuous screw extruders. Total power, motor power, and melt temperature profiles were analyzed in an industrial scale single-screw extruder. Moreover, the active power (AP), mass throughput, torque, and power factor were measured in a laboratory scale twin-screw extruder. The results confirmed that the specific energy consumption for both single and twin screw extruders tends to decrease with the processing speed. However, this action deteriorates the thermal stability of the melt regardless the nature of the polymer. Rheological characterization results showed that the viscosity of LDPE and PS exhibited a normal shear thinning behavior. However, PMMA presented a shear thickening behavior at moderate-to-high shear rates, indicating the possible formation of entanglements. Overall, the findings of this work confirm that the materials' rheology has an appreciable correlation with the energy consumption in polymer extrusion and also most of the findings are in agreement with the previously reported investigations. Therefore, further research should be useful for identifying possible

Abbreviations: AP, active power; BF, barrier flighted screw; GC, gradual compression screw; LDPE, low density polyethylene; LLDPE, linear low density polyethylene; MVR, melt-volume flow rate; MWD, molecular weight distribution; PET, polyethylene terephthalate; PF, power factor; PMMA, polymethyl methacrylate; PP, polypropylene; PS, polystyrene; RC, rapid compression screw; SSE, single-screw extruder; SSEn, single-screw extrusion; SEC, specific energy consumption; TSE, twin-screw extruder; TSEn, twin-screw extrusion.

This is an open access article under the terms of the Creative Commons Attribution License, which permits use, distribution and reproduction in any medium, provided the original work is properly cited.

© 2020 The Authors. *Polymer Engineering & Science* published by Wiley Periodicals, Inc. on behalf of Society of Plastics Engineers.

correlations between key process parameters and hence to further understand the processing behavior for wide range of machines, polymers, and operating conditions.

KEYWORDS

polymer extrusion, polymer rheology, power factor, process monitoring, specific energy consumption, thermal stability, torque

1 | INTRODUCTION

Extrusion serves as a dominant technique of processing polymeric materials all over the world. Around 50% of the global polymer production involves, somehow, an extrusion process in their manufacturing process.^[1] However, processes demand considerable amounts of energy,^[2-7] mainly due to the traditional processing conditions at which the manufacturers are used to work.^[2,7-10] Mostly, these settings are limited to maintain the quality of the product neglecting the intensive power consumption of the machine. In contrast, the best operating point comprises not only the thermal homogeneity of the polymer melt, but also the energy efficiency of the extruder.^[2,7-10] Usually, the processing conditions which are solely chosen by the operator determine the power consumption in each process. Meantime, the melt viscosity can be considered as the best thermal stability indicator of polymer processes.^[11] Therefore, it is crucial to define the best operating point between power consumption and rheology to ensure both, energy and thermal efficiencies simultaneously.^[2,4,10,12,13] Optimization of polymer extrusion processes remains a challenging task due to the inherent complexity of the correlation(s) between the power consumption and the rheological properties of polymers. However, it is quite important to optimize these processes for many reasons. First, because of the power is expensive and the minimization of operational expenses will help to increase the profit margins of the industrial sector. Second, the optimization can contribute to achieve better production conditions; this means better quality products for customers with optimum use of resources (hence a reduced impact on the environment). And thirdly, real-time studies on the thermal and/or rheological behavior of polymers during extrusion have not been widely reported although a numerous offline studies are available in the published literature. Establishing the best operating point is beyond the scope of this study. However, the study will offer valuable insights into the reduction of energy consumption in the extrusion processes while optimizing the product quality and cost.

Since 1970s, the production of polymers has risen fivefold and continues to rise extremely fast in developing countries such as China and India.^[14] South East Asia (including Japan) and North America are the largest production/consumption zones with a 60% of production

and also with a 62% of consumption globally.^[15] Of the total plastics consumption in Europe, Germany, and UK consumed 28% and 11%, respectively. Moreover, at present polymer industry is one of the major parts of the UK's current economy with a sales turnover of over £23.5 billion (with more than 170 000 employees).^[16] Meantime, PlasticsEurope has quoted "Plastics the material for the 21st century".^[17] The rise of consumption combined with the high prices of the oil has increased the operating cost of polymer process.^[15] Moreover, energy is another factor which contributes to increased cost as energy represents the third largest variable cost in polymer processing industry,^[18] and hence its analysis is exceptionally important and timely for the global market place.

1.1 | Plastication in polymer extrusion

Viscous and frictional heat generations are two main forms of heat sources utilized for plastication in polymer extrusion in addition to the conductive heat provided via barrel/die heaters. Agassant et al^[19] stated that the time required for a polymer on a hot surface to reach the same temperature is extremely long since these materials are poor thermal conductors. Due to this lack of heat transfer performance, polymers become molten at a very slow rate. However, the viscous heat generation due to mechanical operation of the process improves the rate of plastication remarkably.^[20] In extrusion processes, the heat energy is dissipated by the rotation of the screw and the rate of dissipation increases usually with the screw speed. Also, the rate of heat dissipation is linearly proportional to the product of viscosity and shear rate (for Newtonian fluids to $\eta \times \dot{\gamma}^2$ and for non-Newtonian fluids to $K \times \dot{\gamma}^{n+1}$, where K and n are the consistency index and melt flow index, respectively).^[21] Figure 1 is a schematic representation of the shear flow between two parallel plates. For a pure drag flow (when the material is in the solid state), the constant shear rate generates a uniform viscous heat generation. As material starts to melt (due to the externally provided and internally generated heat), the drag flow turns into a viscous-drag flow at the later zones of an extruder.

As was mentioned by Severs,^[22] the correct performance of the plastication process has a positive effect on

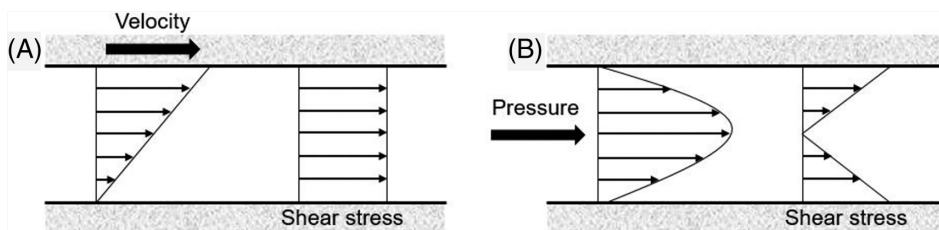


FIGURE 1 A, Velocity and shear stress distribution for Couette flow. B, Pressure and shear stress distribution for Poiseuille flow

the structural, physical, and mechanical development of final polymeric products. In the plasticating region, some of the heat energy is supplied by external heaters. However, the mechanical energy of the rotating screw is the major source of input energy particularly in the feed zone.^[19,20,23,24] This type of energy generates due to the frictional heat between solids in a rapid and homogenous way. The plastication starts with the formation of a thin film of molten material between the barrel wall and the conveyed solids.^[25] This melt film grows in thickness with the rotation of the screw, by viscous dissipation of mechanical energy. When the film is thicker than the flight-barrel clearance, it is compressed against the passive flight forming a recirculating melt pool as shown in Figure 2.

The plastication process is completed when the solid bed disappears, that is, all the solids have melted. Followed by a sequence of experiments, Tadmor et al^[26,27,28] proposed an equation for calculating the melting rate inside a screw channel (Ω) of a single screw extruder and is given in Equation (1).

$$\Omega = \sqrt{\frac{\rho_m V_{bx} [k_m(T_b - T_m) + \eta \frac{V_j}{2}] X}{2[C_p(T_m - T_s) + \lambda]}} \quad (1)$$

Where ρ_m is the density of the melt, V_{bx} is the velocity of the barrel in the transverse direction, k_m is the thermal conductivity of the melt, T_b is the temperature of the barrel, T_m is the temperature at the solid bed-melt film interface, η is the melt viscosity, V_j is the resultant relative velocity, C_p is the specific heat capacity of the solid bed of the polymer (which is at a constant pressure), T_s is the temperature of the solid bed, X is the width of the solid bed and λ is the heat fusion of polymer. Despite the complexity of this equation, it has been demonstrated that increasing the screw speed (via V_j) can improve the melting rate and this fact has been proved by experiments as well.^[20] However, at high speeds, the residence time of the polymer within the barrel is short which means less time for heat conduction and consequently a less thermal homogeneity due to the possible delays in melting.^[20,21] Hence, at high speeds, partially molten materials may present with the throughput and hence the selection of appropriate process settings (mainly the rotational speed and barrel/die set temperatures) is crucial for achieving

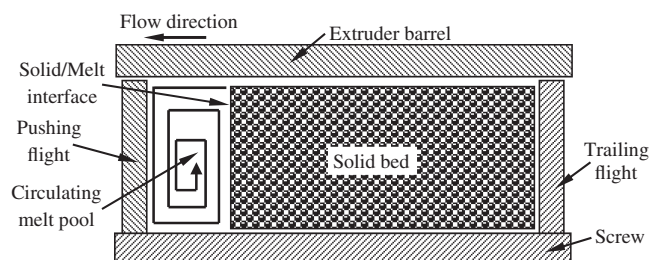


FIGURE 2 A schematic showing the solid bed and melt pool in a screw channel of a single-flighted screw

good quality melt. Consequently, the effectiveness of the plastication is dictated by the melting rate which should be managed by a homogeneous heat supply. However, heat energy available for melting depends on the processing conditions, material being processed and the nature of the processing machine.

1.2 | Energy consumption in polymer extrusion

The energy required in an extrusion or any other process is associated with the economic as well and environmental factors. CO₂ emissions cause an irreversible impact to the environment while the increased energy bills reduce the profit margins for producers and hence, increase the end product prices for customers. Consequently, it is important that the development of a framework which allows measuring, managing, predicting, and minimizing the energy required for the polymer processing industry. The extrusion process is a polymer conversion technique with a sequence of three main functional steps: melting of the solids, forming into a desired shape and solidification of the final product. Melting (or plastication) is the greatest energy demander in comparison with the low mechanical energy required for forming and cooling. Here, the drive motor and the heating system are the major energy consumers. For this reason, it is important to analyze not only their power consumption, but also the losses. Unfortunately, these values cannot be quantified in general and will depend on the specific characteristics of the machine, material being processed and the operators' experience. Severs^[22] proposed an energy flow diagram for polymer extrusion as presented in Figure 3.

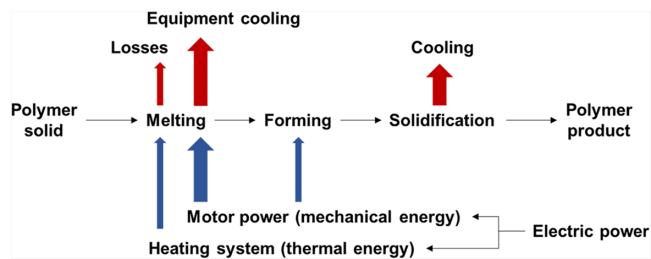


FIGURE 3 Energy flow diagram for a typical extrusion process^[29] [Color figure can be viewed at wileyonlinelibrary.com]

Due to the remarkable increase of demand for polymer products over the last few decades, production rates have been a major concern of manufacturers to cater customer demand with good quality products while achieving their profits. However, no major concern has been shown for energy efficiency of polymer extrusion processes over the past few decades but the recent increase in energy costs and the predicted limitations of energy sources for the future use has forced all the energy intensive processes to critically think about their energy usage and the carbon footprint. An optimum overall efficiency is not only focused on the energy efficiency of the machine, but also on the thermal quality of the polymer melt.^[7,30,31] Thermal quality/efficiency means that the melt temperature should be homogeneous over the time and also across the melt flow cross-section.^[19] Hence, the melt temperature must be controlled from the feeding section to the metering section in an appropriate level(s) by manipulating processing speed and barrel/die set temperatures. In this way, polymer product manufactures should be able to aim for high-quality products at a low unit cost. Many previous studies^[32] have been focused to calculate the energy efficiency of extruders (ie, the typical demand and losses associated with components). However, no much attention has been paid to study both thermal and energy efficiency simultaneously although these two factors seem to be coupled in a complex manner.^[33-36] Hence, this work aims to extend the level of understanding in this research area by observing both energy and thermal parameters with a series of properly designed system identification experiments.

1.3 | Rheology in polymer extrusion

Polymer melt rheology studies the deformation and flow behavior of polymeric materials in the molten state. Rheological characteristics are unique for each type of polymer and vary according to processing factors such as shear rate, melt temperature, and melt pressure.^[37,38] Inside a hot barrel of an extruder, the viscosity may be

studied by the resistance of the polymer to flow.^[22] Some polymer properties such as the molecular weight, the molecular weight distribution (MWD) and the molecular configuration control the viscous behavior of the melt. For example, more entanglements means a greater resistance to the flow and also the polymers with high molecular weight present high viscosities.^[39] Similarly, modifying the MWD affects the elasticity of the melt,^[40] meaning that polymers with a broader MWD exhibit greater variations in the viscosity when the shear stress increases.^[12,41] Moreover, molecular configurations act as an energy barrier against the flow, reducing the chain flexibility and its rotation.^[38,40] Hence, thermal and rheological behavior of polymer melts should be analyzed together with the energy demand to achieve an optimum overall efficiency for a given machine and a material.

1.4 | Effect of energy consumption and rheology on extrusion process efficiency

In recent years, there has been an increase in research in the areas of process monitoring, modelling, optimization, and control for determining the best possible operating point for extrusion processes particularly for achieving the best possible energy efficiency from these processes. Some of these researches attempted to link the energy consumption with the processing conditions of extruders while only a limited amount of research have explored the relationship(s) between the power consumption, process settings, and the rheological characteristics of polymers.

Kelly et al^[32] used a novel temperature sensor consisting of a thermocouple mesh to measure the melt temperature, melt pressure, and power consumption in real time for both single and twin screw extrusion process. This device was developed, validated and calibrated in a previous study by Brown et al.^[42] A low density polyethylene was processed in a single screw extruder with three different extruder screws in a range of screw speeds. The authors reported that the screw geometry plays an important role over the melting performance and stability of the melt flow. At high throughputs, a barrier-flighted screw provided significantly better melting conditions, lower variation in the melt pressure and temperature than conventional single-flighted screws.

Abeykoon et al^[33] investigated the motor power consumption in a direct current (DC) motor of a single-screw extruder by modelling the effects of operating conditions. The study determined a new static nonlinear polynomial model to predict the motor power consumption while varying processing conditions and materials. The authors identified the screw speed as the most influencing

parameter to achieve a higher motor energy demand. Conversely, varying the barrel set temperature only caused a slight effect in the motor energy consumption. Another work by Abeykoon et al^[10] defined the melt pressure as an important parameter in process optimization and hence the product quality. The results demonstrated that the melt pressure generation is influenced by the individual process settings and the screw design. The processing parameters should be selected according to the screw geometry to reduce possible conveying problems and therefore the possible melt pressure fluctuations.

In 2011, Abeykoon et al^[43] studied the torque dynamics of an extrusion process via an inferential monitoring approach. This torque signals are thought to be an important indicator of process fluctuations, that is, stability during conveying, melting, mixing, and so on. The results established that high values of torque correspond to solid polymers with high frictional properties. However, this research had not been able to determine a possible correlation between the melt temperature and torque, due to the weak correlation of the signals between these parameters.

Deng et al^[3] explored the viscosity as a fundamental indicator of melt quality in an extrusion process. A soft-sensor was used to develop a model which enables to monitor the viscosity. According to this study, the viscosity is very sensitive to changes in the melt pressure. A variation of 0.1 MPa in pressure may lead to a 16 Pas change in viscosity. In another work, Deng et al^[11] developed simple and accurate monitoring methods to analyze the energy consumption of the motor and the thermal heating system. The results exposed that the energy efficiency is negatively correlated with the set temperature of the barrel, and positively but insignificantly with the water cooling system. Therefore, the lowest specific energy consumption (SEC) of the extruder can be achieved only with low barrel heating temperatures and high water cooling temperatures at high processing speeds.

Furthermore, Deng et al^[4] developed a few process monitoring methods to determine the effects of process settings on energy and thermal efficiencies. Their experimental results confirmed that the energy efficiency could be improved by changing the processing conditions. For example, a low barrel heater setting is preferred due to high barrel temperatures may lead to a high heater energy consumption and a low motor energy consumption, with an increase in the total SEC. Screw speed has an important impact on SEC of heaters/motor and the melt quality. For instance, this research suggested that setting a high screw speed would be good to achieve a higher energy efficiency, better melt stability, and also a

higher throughput. On the other hand, the authors suggested a few methods to maintain the melt consistency: use of a rule-based fuzzy controller to keep the melt pressure and the melt temperature at the desired levels, and also to adopt the viscosity as the best melt quality indicator.

According to Abeykoon,^[44] in a typical extruder, the drive motor and the heaters are the first and the second largest energy consumer devices, respectively. Abeykoon et al^[2] analyzed various processing conditions to identify the best way to optimize the total energy efficiency in an extrusion plant. The investigations confirmed theoretically and experimentally that the screw speed and the material being processed are the parameters with the greatest influence on the total energy demand. However, energy and thermal efficiencies can only be achieved simultaneously by studying correlations between extruder processing settings and material properties. However, the authors mentioned that forming of such correlations should be highly complex. Another work by Abeykoon et al^[30] showed that the SEC and the energy demand fluctuations decrease with increasing throughput regardless the screw geometry. However, unfortunately, increasing the throughput damaged the melt thermal stability of the polymer, concluding that energy and the thermal efficiency are negatively correlated.

Vera-Sorroche et al^[45] used an infrared temperature sensor to quantify the thermal homogeneity of a HDPE polymer melt without disturbing the flow. This sensor was located in the metering section of the barrel and allowed to obtain real-time data during processing. Comparisons were made with their previous work^[46] and showed similar results. The analysis of the data reported that high viscosities imply high SEC, poor melt homogeneity and large fluctuations in radial melt temperatures. This study confirms previous investigations^[7,31] regarding the correlation between processing settings, energy consumption and polymer molecular weight.

Recent investigations of Abeykoon et al^[12] focused the attention on the comparison of energy consumption of semicrystalline and amorphous polymers. The results revealed how the variation in MWD and the degree of branching affects the SEC of extruders. Additionally, a possible correlation between the thermal stability and the energy consumption of the heaters was suggested. However, the authors recommended investigating this fact thoroughly before giving exact conclusions. Meantime, the same authors have reported some other researches recently on how to improve the processing performance by improving process monitoring and control.^[47-52] Furthermore, a few other works have focused on improving the process efficiency by optimizing the screw performance^[53,54] and also using other software/hardware tools

for optimizing the process settings.^[55-59] Although, these works are really important in terms of process developments, more details on such works are not presented as it is out of the main focus of the current research.

In general, the majority of above mentioned studies clearly indicate that there is a relationship between process settings, the material properties and the energy consumption in single-screw extruders. However, the complex correlations of these factors in twin-screw extruders has still remained significantly unclear while only a little progress has been made in understanding the area of single-screw extrusion. Therefore, it is timely important and commercially necessary to evaluate this major field relating to both single and twin screw extruders as both types are really important in the processing of polymeric materials and this study aims to fill these gaps through widening the understanding on the state-of-the-art of processing behavior. Moreover, this study investigates the possibility of scale-up (or scale-down) to link the processing behavior between laboratory and industrial scale machines in polymer extrusion. This is also an area only a very little research has been reported so far. Most of the laboratory machines are well-equipped for carrying out for system identification experiments but it would be extremely difficult to perform those types of tests on real industrial scale extruders. Hence, establishing those links between laboratory and industrial scale machines would be invaluable for the development of polymer processing industry. Furthermore, this study aims to make a comparison between the processing behavior of single-screw and twin-screw extruders. Such a detailed investigation on process scale-

up/down, process energy demand, melt thermal quality, melt rheology over wide range of materials, screw geometries and processing conditions is not available in the published literature.

2 | EXPERIMENTAL

Experimental work in this study considered a medium scale 63.5 mm diameter single screw extruder (Davis Standard BC-60) available at Polymer IRC at University of Bradford and a small scale corotating twin screw extruder (Haake MiniLab) available at the North West Composites Centre at the University of Manchester. These two types of extruders were selected as these are the most commonly used types in industry. The major part of the experiment was performed on the Haake MiniLab while some of the results previously presented by Abeykoon et al^[2,8,12,46] relating to the same BC-60 single screw extruder was used in this study for comparison purposes.

2.1 | Experimental equipment and procedures

2.1.1 | Single screw extruder

With the BC-60 single screw extruder (SSE), three screws (gradual compression [GC], rapid compression [RC], and a barrier flighted [BF]) were used with five different materials (details are given in Figure 4 and Table 1). The screw speed was increased from 10 to 90 rpm in the

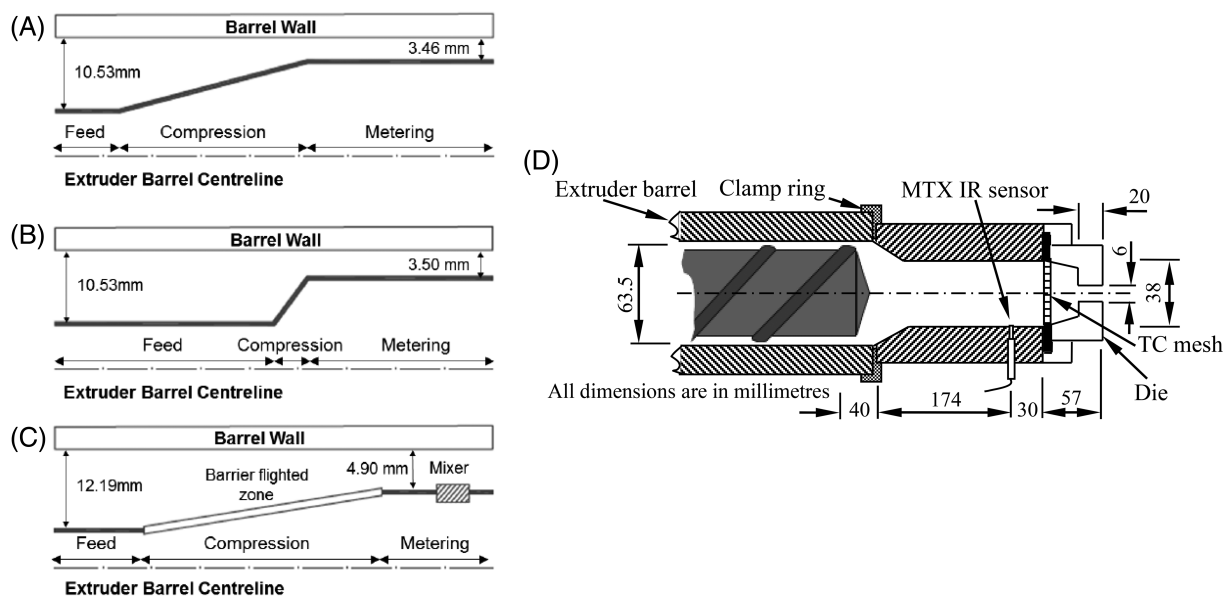


FIGURE 4 Geometrical details of single screws used in the experiment, A, gradual compression screw, B, rapid compression screw, C, barrier flighted screw, D, Dimensions and the arrangement of the experimental apparatus

Test	Temperature settings (°C)				Clamp ring	Adapter	Die	Material
	1	2	3	4				
A	130	155	170	180	180	180	180	LDPE, LLDPE, PS
B	140	170	185	200	200	200	200	
C	150	185	200	220	220	220	220	
A	240	260	280	280	280	280	280	PET
B	250	270	290	290	290	290	290	
C	260	280	300	300	300	300	300	
A	140	170	185	200	200	200	200	PP
B	150	185	205	220	220	220	220	
C	150	185	220	240	240	240	240	

TABLE 1 BC 60 SSE barrel temperature settings

intervals of 20 rpm. As given in Table 2, three set temperature conditions: Low (A), medium (B), and high (C), were set to the barrel, clamping ring, adapter and die during the experiments. The arrangement and the dimensions of the extruder barrel, clamp ring, adapter, and die are shown in Figure 4D.

The set temperature conditions of each material were selected to cover their processing window. The SSE used a Hioki and an Acuvim IIE 3-phase power meters to measure the total power and motor power, respectively. Additionally, all the signals were monitored in real-time at 10 Hz via a data acquisition program developed in LabVIEW.

2.1.2 | Twin screw extruder

In a similar way, nine experimental trials were carried out using the Twin screw extruder (TSE) MiniLab Micro-Compounder, manufactured by Haake Company, Germany. The heating system comprises four heating bands of each 200 W. The screw speed range is between 0 and 360 rpm and the maximum torque per screw is 5 Nm. The motor was manufactured by the Creusen Roermond

Holland, The Netherlands. Characteristics of the motor are displayed in Table 2.

As shown in Figure 5, this TSE was equipped with two stainless steel (1.4122) conical screws inside the barrel made of a high-performance plastic mould steel (M340). The total capacity of the barrel and the recirculating channel is 7 mL. Additionally, the position of the spring arm and the gear wheel alignment were adjusted to make the machine work as a corotating twin screw extruder.

In TSE, the total current, active power (AP) and power factor (PF) were measured using a VIP96 power meter, devised by ElControl Energy Net, Italy. These data were recorded manually in every 15 seconds during the processing experiments. The MiniLab TSE with the power meter is shown in Figure 6.

The experimental procedure used with TSE was also selected by following the same criteria employed with the SSE. Three different polymers used (LDPE, PS and PMMA) and set temperatures used with them, A: low, B: medium, and C: high, are presented in Table 3.

The maximum motor torque measurements were recorded in every 15 seconds. The maximum load was needed to obtain the maximum torque,^[13,32,35] hence the

Creusen Roermond Holland motor					
Characteristics	71SSH-2GPFPP/239			N°	562 680
Power (kW)	0.15	RPM	1500	FF	1.05
Arm V	24	Arm A	1.5	Ins. CI	F
Exc. V	P	Exc. A	max = 4.8	Amb. °C	40
Duty	S1	Cool IC	4A1A0	Prot. IP	54
Mount FM	3601	Mass Kg.	7	Choke	

TABLE 2 Haake MiniLab motor plate

FIGURE 5 Haake MiniLab: A, Internal extruder housing, A.1, Backflow channel, A.2, Pressure sensor, A.3, By-pass valve, A.4, Extrusion channel. B, Internal drive unit [Color figure can be viewed at wileyonlinelibrary.com]

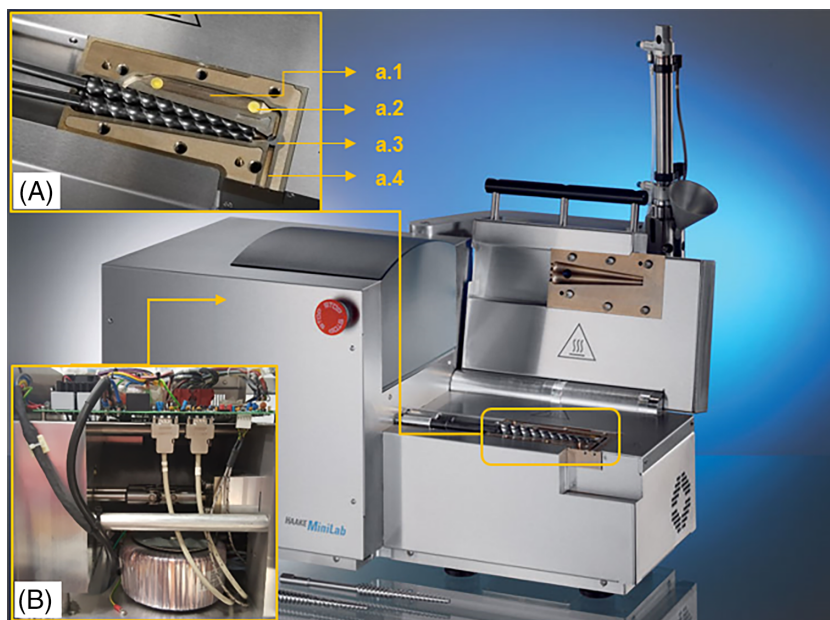


FIGURE 6 Twin-screw extruder with other experimental equipment. A, Power meter, B, Interface control system, and C, Haake MiniLab [Color figure can be viewed at wileyonlinelibrary.com]

optimum feed quantities in the 7 mL channel were 6 g for LDPE, 7 g for PS, and 8 g for PMMA, per batch. Data was recorded for 10 minutes at 10 rpm and then for 5 minutes at the rest of the screw speeds, with 1 minute of stabilization time between each change of speed.^[2,7,8,10,30-32] Mass throughput performance was measured by loading the extruder with the maximum feeding quantities for each material.^[13,20,43,60] The material was kept recirculating for 10 minutes to assure thermal homogeneity. After this

TABLE 3 The experimental set temperatures used with twin screw extruder for each material

Temperature (°C)	Material		
	LDPE	PS	PMMA
A	180	180	210
B	200	200	230
C	220	220	250

time, the flush valve was activated, and the amount of polymer collected for 1 minute was weighted to obtain the output per unit time.^[61]

2.2 | The experimental materials

Altogether, industrially common six commodity grade thermoplastics were used in this study and more details on these materials are presented in Table 4. Also, these materials were selected to study the behavior of both crystalline and amorphous polymers. Only PMMA was required to be pre-dried at 75°C for at least 24 hours prior to start the experiments while other five materials were used as they were received from the manufacturer. Moreover, the set conditions used for rheological studies are presented in Table 5.

2.3 | Polymers characterisation

For rheological testing, Virgin PMMA, LDPE and PS pellets were processed by compression moulding to obtain discs of 25 mm diameter of 1 mm thickness. These samples were tested in a Discovery RH-3 TA Instruments rheometer as shown Figure 7. Two types of test were carried out under parallel plate-plate configuration: the steady shear test (sweep-flow) and the dynamic shear test (oscillatory sweep-flow). To ensure the thermal equilibrium, the samples were placed over the plate at the set temperature (Table 3) for 10 minutes before starting the experiment.^[62] The gap between plates was adjusted to 1 mm to ensure a uniform flow and shearing.^[38]

TABLE 4 Details of the polymeric materials used in experiments

Polymer type	Trade name	Grade	Manufacturer	Density	Melt flow rate (MFR)		Melt volume-flow rate MVR	
				(g/cm ³)	(g/10 minutes)	(g/10 minutes)	(cm ³ /10 minutes)	
LDPE	Lupolen	2420 H	LyondellBasell	0.924	1.9	190°C/2.16 kg	-	-
LLDPE	Flexirene	CL 10	Versalis S.p.A.	0.918	2.6	190°C/2.16 kg	-	-
PP	Moplen	HP640J	LyondellBasell	0.9	3.2	230°C/2.16 kg	4.3	230°C/2.16 kg
PET	PET	D717A	Edinburg plastics	1.34	-	-	-	-
PS	Styrolution	PS 124N	Styrolution	1.04	-	-	12	200°C/5 kg
PMMA	Plexiglas	8N	Plexiglas	1.19	-	-	3	230°C/3.8 kg

Each trial was carried out under the same set temperature conditions used with the TSE to process the materials. The strain rate was kept within the linear viscoelastic regime (10^{-1} - 10^2 seconds⁻¹)^[63] and the angular velocity from 0.1 to 10 rad/s (0.9-95 rpm). Shear viscosity and torque were recorded by the steady shear test. Moreover, the complex viscosity, the storage modulus and the loss modulus were obtained by the dynamic shear test with an angular frequency range of 0.1 to 628 rad/s.^[62]

The recirculating time was chosen to assure the thermal homogeneity, but at the same time to avoid possible thermal degradations. For this purpose, a number of pre-trials were carried out by varying the recirculating time prior to the proper experiments and the melt output was visually observed for un-malted particles and for possible degradation indicated by the color changes. After this time, the flush valve was activated, and the extrudate was collected over a metal plate without pulling. This procedure allowed causing minimal disruption to the normal extrudate flow.

2.4 | Physical analysis of the extrudate

The data obtained from the TSE was used here. LDPE, PS and PMMA were weighted with their optimum feed quantities, in order to work with the maximum volume of the barrel.^[13,43,60] Each material was processed at minimum (MIN), intermediate (INT), and extreme (EXT) conditions. Table 5 provides the detailed information of these settings.

3 | RESULTS AND DISCUSSION

3.1 | Minilab electrical system

The Haake MiniLab TSE is a miniaturized high-tech machine perfect for investigations in material science. Some of the previous studies^[60,61] have confirmed its

TABLE 5 Set conditions used for rheological and physical analysis of the extrudate

	LDPE and PS			PMMA		
	Minimum MIN	Intermediate INT	Extreme EXT	Minimum MIN	Intermediate INT	Extreme EXT
Feed quantity (g)	6 for LDPE	7 for PS (for all three conditions)		8 (for all three conditions)		
Temperature (°C)	180	200	220	210	230	250
Screw speed (rpm)	10	90	300	10	90	300
Recirculation time (min)	5	7	10	5	7	10

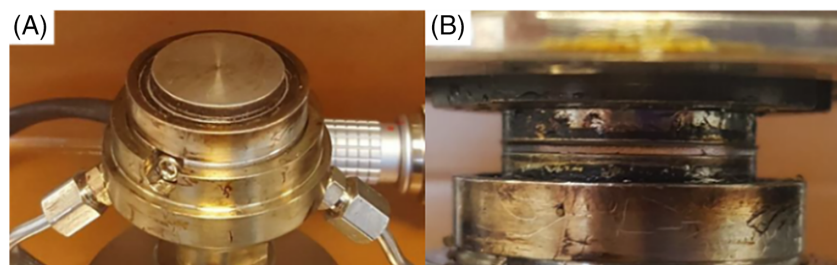


FIGURE 7 Rheometer plates: A, Lower plate without sample and B, sample in between the plates [Color figure can be viewed at wileyonlinelibrary.com]

excellent functionality as a normal TSE. However, in the course of this research, it was felt that it is necessary to analyze its electrical system's operation. This is due to the energy consumption of any machine will depend solely on the operational behavior of its components. Moreover, this analysis should be useful to consider if the electrical comparison between this laboratory instrument and the 63.5 mm diameter industrial scale SSE is appropriate or not.

3.1.1 | Initial heat-up

First, current, active power (AP) and power factor (PF) were measured as the extruder was turned on at room temperature until it reached the set temperature of 250°C (with no motor running) and the measured signals are shown in Figure 8.

This MiniLab TSE has four heater bands (each of 200 W), and the measured power signal confirms that the machine occupies all the heaters in the initial heat-up, and demands around 60 W of additional power for the display and the other control electronics. It is evident that the PF remains 1 of up to 1200 seconds until all the heaters reach their set temperature (the dashed line shows a gradual increase of set temperature). This behavior is because commonly the heaters are resistive loads, which keeps the PF at unity^[2] and makes the machine works in its best operating conditions in terms of energy consumption.^[12] As the barrel heaters reached the set temperature, three heaters went off and then the AP reduced to 260 W. As was explained previously by Kruder and Nunn,^[6] the barrel heaters demand a relatively high energy (in addition to the drive motor) than the rest of the components in an extruder.

3.1.2 | Response to the set temperature changes

The same parameters were recorded since the machine was turned on until it reached the set temperature of

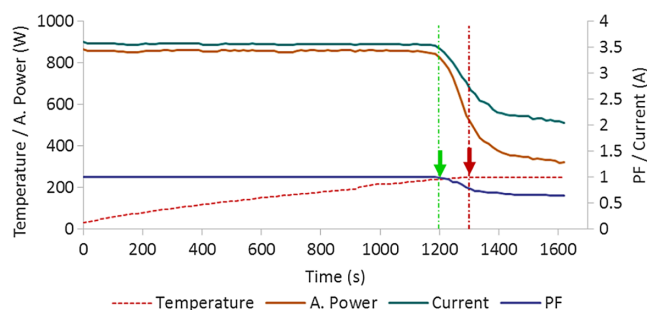


FIGURE 8 The measured electrical parameters of Minilab twin screw extruder during the initial heat-up (with no motor running) [Color figure can be viewed at wileyonlinelibrary.com]

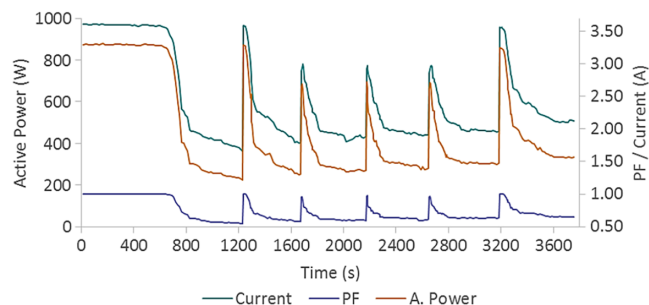


FIGURE 9 The measured electrical parameters of Minilab twin screw extruder during the barrel set temperature changes (with no motor running) [Color figure can be viewed at wileyonlinelibrary.com]

180°C. And then the barrel set temperature was increased gradually from 180, 200, 210, 220, 230, and 250°C, which are the set temperatures used to process the different polymers. The signals observed are shown Figure 9. It can be seen that the PF reaches the unity as heaters turned-on and then reaches to a value of around 0.55 when they are switched-off. Abeykoon et al.^[2] argues that the set temperature changes cause the vector sum of impedance to become resistively dominant and hence the PF rise to the unity as a change of set temperature was applied.

3.1.3 | Response to the motor speed changes

Here, the current, AP and PF were measured while increasing the screw speed from 0 to 300 rpm in intervals of 50 rpm and the signals observed are shown in Figure 10. The barrel temperature was set to 180 °C with a load of 7 g of LDPE inside the barrel.

These curves show that the AP has increased with every change of speed. A small peak (caused by the disturbance/resistance in changing the processing conditions) appears in the curves with every change of speed but it stabilizes rapidly. In the other hand, when the motor stops suddenly, a big drop of power can be observed. However, the values start to increase instantaneously and stabilise due to the increased energy demand by heaters.

For this particular type of a TSE, the motor does not consume the highest proportion of the total energy due to the small wattage at which it works. This fact contradicts what previous studies^[2,12] have demonstrated for SSEs, however this is purely due to the size of this particular TSE (a small motor can provide the rotation of screws of this MiniLab TSE). As a MiniLab TSE of this scale has not been designed for production purposes, its

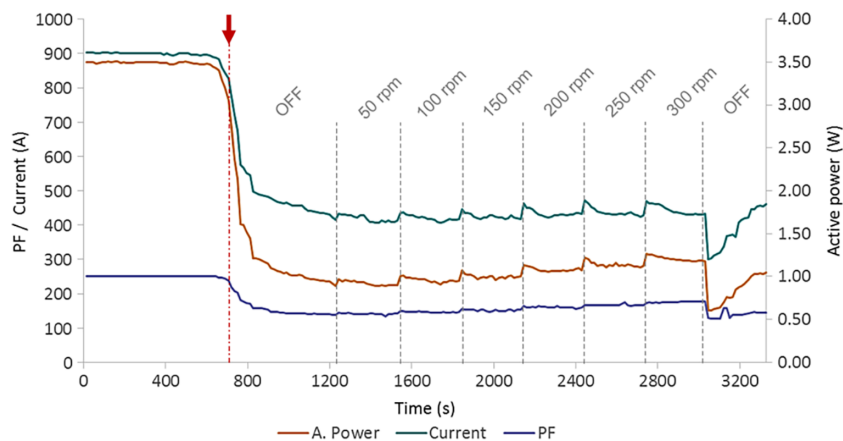


FIGURE 10 The measured electrical parameters of Minilab twin screw extruder during screw speed changes from 0 - 300 rpm [Color figure can be viewed at wileyonlinelibrary.com]

motor power consumption cannot be compared with large scale industrial TSEs or SSEs. Consequently, in this work, the total energy consumption will be analyzed and compared in a general perspective.

3.2 | AP demand of TSE with different materials

The AP consumption of TSE was monitored for LDPE, PS, and PMMA materials. Figure 11 shows that the AP demand of the TSE rises erratically with the screw speed despite the material being processed and the processing conditions which is a similar behavior to industrial scale extruders.^[2] However, these fluctuations are strongly influenced by the type of the polymer and the barrel/die set temperature. It is noticeable that the machine needs more power to process PMMA than the other two materials. This might be attributed to the restrictions on the flow properties caused by bulky side groups of PMMA: the methyl and the methacrylate.^[23,41,64] These molecular configurations act as an energy barrier against the flow, reducing the chain flexibility and rotation.^[38,40] Therefore, a high level of mechanical energy should be applied in order to activate the flow. Moreover, these large side groups not only affect the deformation of the melt, but also increase the effect of temperature on the melt viscosity.^[22]

Similarly for PS, at low temperatures when the free volume is limited, the toluene restricts the flexibility of the chains^[39] causing highly fluctuating processing behaviors. In general, PMMA and PS are temperature sensitive materials at high temperatures and hence they show a decrease in the rate of melting^[20] and consequently the magnitude of the fluctuations becomes slightly less as the temperature increases. This cannot be seen with LDPE which exhibits a more stable behavior to the temperature changes.

Previous work by Abeykoon et al,^[2] the total power of the same SSE was also measured while processing a PS (the same PS material used with the TSE) at the low

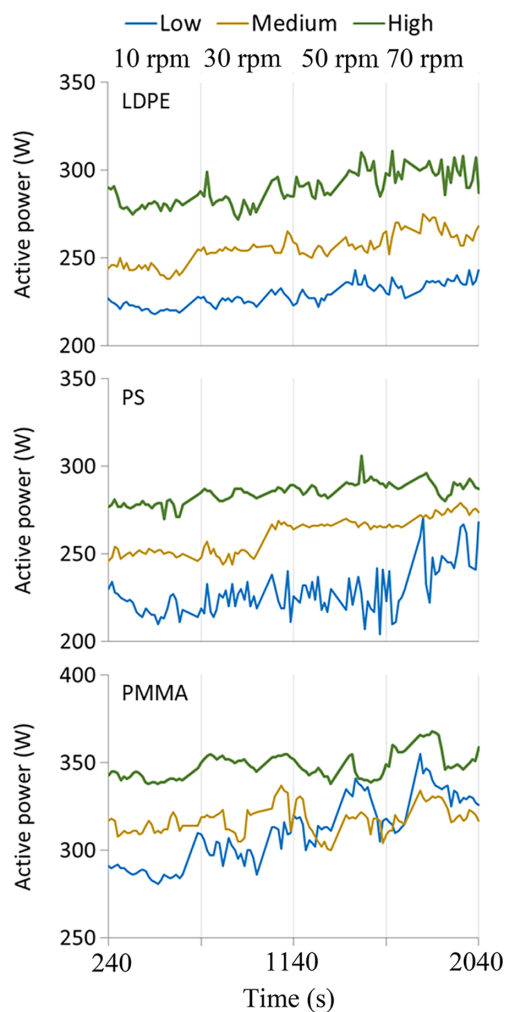


FIGURE 11 Active power variations with screw speed for LDPE, PS, and PMMA for the MiniLab twin screw extruder [Color figure can be viewed at wileyonlinelibrary.com]

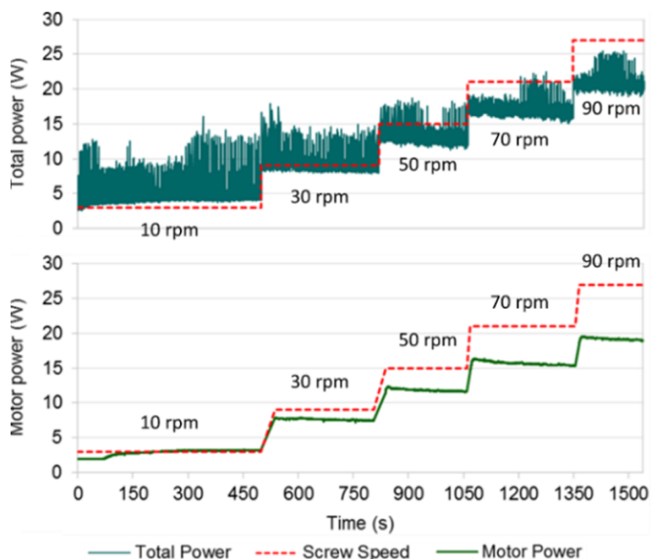


FIGURE 12 Total and motor power characteristics of the single screw extruder with a gradual compression screw (for PS and set temperature condition A) [Color figure can be viewed at wileyonlinelibrary.com]

temperature condition (A) with a GC screw. As shown in Figures 11 and 12, the nature of the total power demand with the screw speed is quite similar for both TSE and SSE (ie, power increases with the screw speed). However, the magnitudes of increments and the level of fluctuations are different as was expected mainly due to the differences of size of the components of these two machines.

3.3 | Mass throughput

The mass throughput was measured experimentally over low (A), medium (B), and high (C) temperature set conditions at different screw speed and screw geometries with both SSE and TSE. Previously reported data shows that regardless the material and the set temperature condition used, the throughput increases as the screw speed increases.^[2,32] This suggests that higher flow rates can be achieved only at higher screw speeds.^[4] According to the greatest throughputs obtained, in Figure 13, the mass throughput tends to increase quite linearly as screw speed increases with SSE while the TSE shows a slight nonlinearity.

As was reported by most of the previous works,^[3,12] the throughput is linear with the screw speed regardless the set temperature, the screw geometry or the polymer being processed for SSEs. Moreover, the rheology of the polymer also plays an important role in the production of polymeric components.^[7,12,32] Dealy^[23] supported this

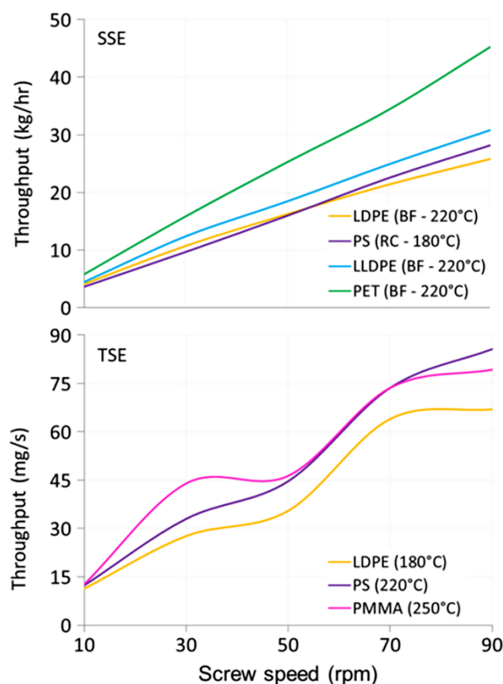


FIGURE 13 Mass throughput with the screw speed with various polymers: single screw extruder (top) and twin screw extruder (bottom) [Color figure can be viewed at wileyonlinelibrary.com]

statement by suggesting some other possible factors such as the melting and pumping capacity of the extruder, the shape of the die and its curvature.

For Minilab TSE, the mass throughput stabilises between 30 and 50 rpm which may be due to an inconsistency and this data is in disagreement with the volumetric flow rate reported by Yousfi et al^[61] who reported a linear behavior. Obviously, the output of an extruder is highly dependent upon the melt pressure^[10,20,40,41] and variations in the melt pressure can cause unstable mass throughput rates,^[3] hence there is an obvious problem of feeding or conveying of the material in TSE. Therefore, this problem may be solved by adding an automatic feeder and also monitoring the process pressure during the process would also be useful in detecting possible mass throughput variations. In a previous work reported by Abeykoon et al^[13] for the same SSE, the mass throughput of a commodity grade of a HDPE stabilised with low values between 10 and 30 rpm which was caused due to the poor melt pressure in that range of speed and hence poor conveying performance was noticed.

3.4 | Specific energy consumption

The extruder SEC was calculated based on the experimentally measured data at low (A), medium (B), and

high (C) set temperatures and at different screw speeds. The SEC is referred to the energy consumed by an extruder to produce a unit mass of extrudate. In both cases, the results of the SSE indicate that regardless the screw geometry,^[7,32] the SEC for all polymers decreases as screw speed increases.^[2,8,32,46] However, some previous work with cyclic block copolymers reported that the SEC increases as the screw speed increases.^[64] However, this is mostly a special case due to the intrinsic properties of these type of polymers.^[2] The experimentally measured SEC relating to a semicrystalline (LDPE) and an amorphous (PS) polymer are presented in Figure 14.

Polystyrene shows the lowest SEC among all the materials used with SSE. This could be explained by the lower softening point of this amorphous material compared with the semicrystalline materials.^[12] The highest SEC was reported with the RC screw for LDPE while for PS it was with the GC screw. Kelly et al^[7] have studied the effects of screw geometries on SEC on the same SSE with a HDPE and found that the SEC decreases with the screw speed. Moreover, they have noticed some effects of barrel set temperature on the SEC but these are minor compared to the effects of the screw speed.

The SEC values obtained with the MiniLab TSE during processing of LDPE, PS, and PMMA are summarized in Figures 15 and 16. Alike the SSE, the TSE also shows a decreasing trend of specific energy demand as screw speed increases although the set temperature does not show a significant effect on these variations.^[12] However,

the SEC is minimum between 30 and 50 rpm which is due to the lower mass throughput achieved. Since, the SEC is the total input power divided by the mass throughput, this behavior can be associated with the pressure instability of the MiniLab without an automatic feeder, as was explained in Section 3.3. A possible explanation for achieving a high SEC at low set conditions (ie, low set temperature and speeds) would be that materials remain highly viscous compared to high set conditions. Hence, the resistance to flow remains high, demanding a higher torque from the motor and while resistive heating become dominant against frictional and viscous heat.^[65]

3.5 | Motor torque

The motor torque was also monitored with the TSE for LDPE, PS, and PMMA under different processing conditions and relevant details are shown in Figure 17.

As it can be observed, the curves show step increments of torque as screw speed increases regardless of the polymer being processed. The maximum torque for LDPE, PS, and PMMA are 65, 80, and 220 Nm, respectively. In each condition, minor fluctuations can be seen, which become slightly bigger as temperature rises. This has been attributed to the poor temperature control in the barrel.^[40,66] On the other hand, another important effect may contribute when the shearing forces act over

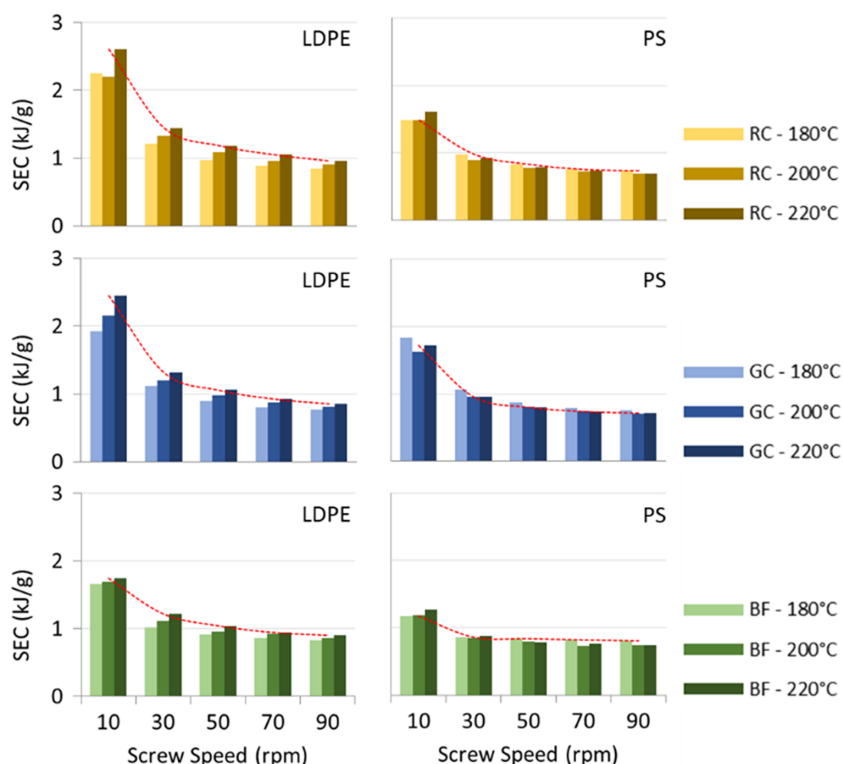


FIGURE 14 Specific energy consumption for LDPE and PS with the single screw extruder with different screws and processing conditions^[8] [Color figure can be viewed at wileyonlinelibrary.com]

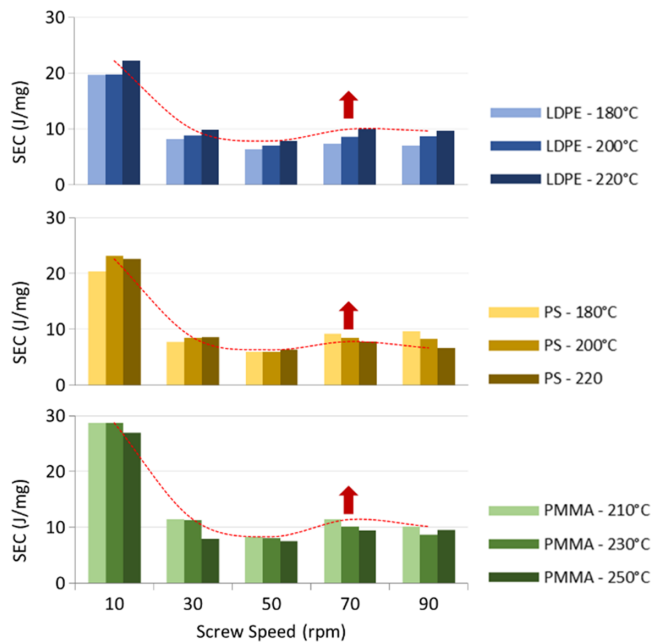


FIGURE 15 Specific energy consumption with the MiniLab twin screw extruder at different processing conditions: LDPE (top), PS (middle), PMMA (bottom) [Color figure can be viewed at wileyonlinelibrary.com]

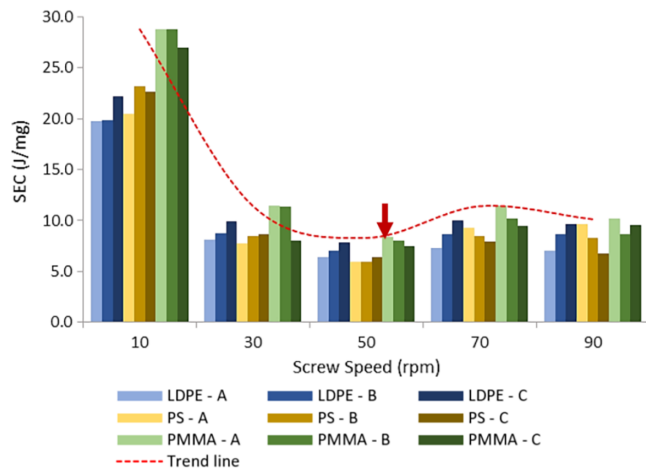


FIGURE 16 A comparison of the specific energy consumption (SEC) of the MiniLab twin screw extruder at different processing conditions for LDPE, PS, and PMMA [Color figure can be viewed at wileyonlinelibrary.com]

the solid bed, it might break-up prematurely causing torque variations.^[13] Therefore, the highest torque values and torque fluctuations presented for PMMA might be due to the same reason affecting the AP discussed in Section 3.2. Therefore, it suggests that the torque and AP demand show a similar behavior with the set conditions, as was expected.^[43]

Generally, motor torque values present a linear increasing trend with the screw speed.^[60,67] However, the

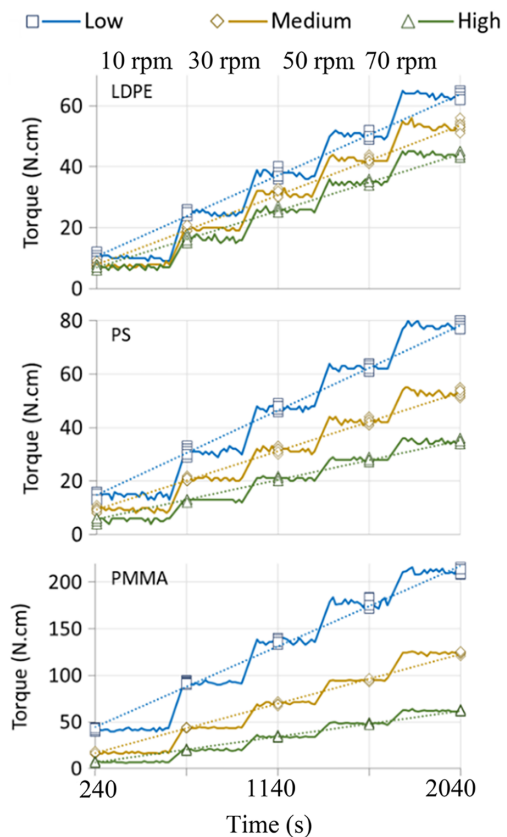


FIGURE 17 Motor torque variations for LDPE, PS, and PMMA at different set conditions [Color figure can be viewed at wileyonlinelibrary.com]

motor torque may not be linear due to the possible varying processing conditions as was observed by Abeykoon et al for a virgin HDPE with the same SSE.^[8] Additionally, the torque data of the experimental rheometer's motor was also observed and presented in Figure 18.

The results show that the torque increases gradually with the angular velocity. In this case, the stepped trend disappears due to the automatic gradual rise in velocity.

3.6 | Power factor (PF)

Figure 19 represents the experimentally measured PF for LDPE, PS, and PMMA with the MiniLab TSE.

Generally, PF increases unsteadily with both the screw speed and the set temperature increments.^[3,4] Normally, the magnitude of the PF is inversely related to the phase shift between the current and the voltage,^[32] as bigger the phase angle the lower the PF is.^[4] In addition, due to the correlation between current-voltage-PF, the power consumption and the energy efficiency are also related to this parameter.^[3,30] Moreover, the higher the PF the better the extruder efficiency is.^[30,32] An

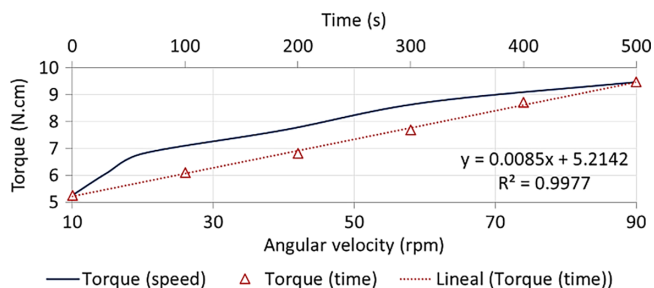


FIGURE 18 Motor torque variations for LDPE at the low temperature condition in a plate-plate rheometer [Color figure can be viewed at [wileyonlinelibrary.com](#)]

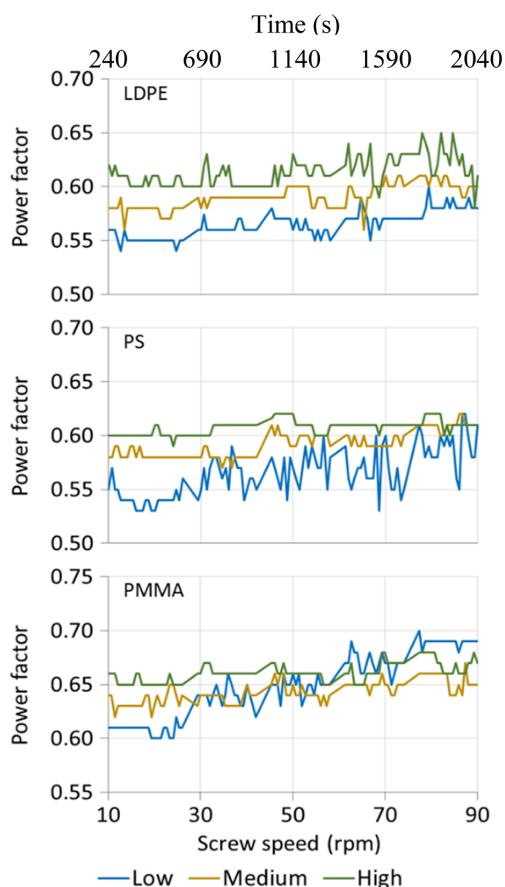


FIGURE 19 Power factor variations for LDPE, PS, and PMMA at different processing conditions with the MiniLab twin screw extruder [Color figure can be viewed at [wileyonlinelibrary.com](#)]

extruder's energy efficiency increases with the screw speed as PF increases.^[12] Of the three polymers used in this study, PMMA shows the highest PF during processing. The PF fluctuations during the processing of LDPE and PMMA are quite the same compared to PS. However, for PS, the high fluctuations indicate that the PF depends on the thermal variations and other

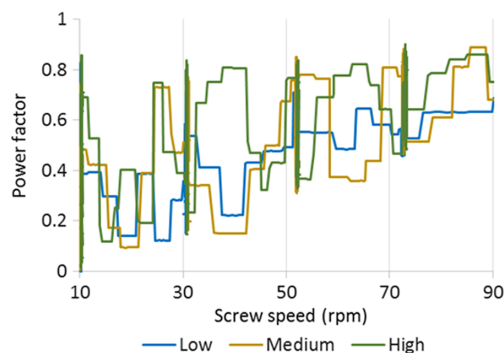


FIGURE 20 Power factor for LDPE at low, medium, and high set temperatures with the barrier flighted screw and a single screw extruder [Color figure can be viewed at [wileyonlinelibrary.com](#)]

material properties as well.^[12] Hence, it is important to mention that the PF does not reach the unity with any of these materials. To achieve the highest PF, all the heaters should be at work (those are resistive components) but this only occurs at the initial heat up of the MiniLab as shown in Figures 8-10. Abeykoon et al.^[12] argues that it is also possible to achieve higher energy efficiencies at higher speeds due to the reduction of SEC, but it would also lead to poor melt quality.

PF was also measured for LDPE with the BF screw using the SSE and the related signals are shown in Figure 20. As the screw speed increases from 10-90 rpm, the PF fluctuates quite a lot as was observed with the TSE as well. However, a highly fluctuating behavior can normally be observed just after the screw speed changes.

3.7 | Thermal efficiency of the melt

A brief analysis of the results obtained previously^[46] with the same SSE is made in this section. A thermocouple mesh was used to monitor the temperature variations across the radial melt flow cross section of the die (38 mm in diameter) entry of the SSE.

3.7.1 | Effects of the screw geometry

Figure 21 shows the thermal variations across the melt flow for LDPE at the set temperature condition A (low) with both BF and GC screws. With both screws, the melt temperature profiles are quite homogeneous from the centre to the radial locations of up to ± 10 mm particularly at 10 and 30 rpm. Here, the melt temperature at the middle of the flow is higher than that of the die wall set temperature by around 20°C . At higher processing speeds

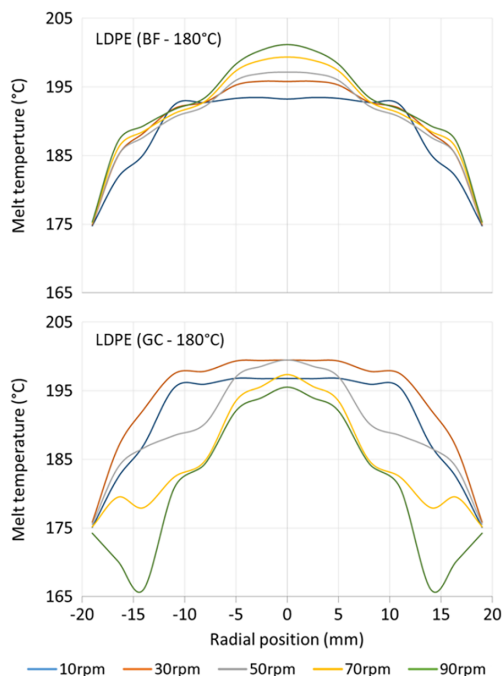


FIGURE 21 Melt temperature profiles for LDPE processed at the low temperature condition (A) with the barrier flighted screw (top) and with the gradual compression screw (bottom) [Color figure can be viewed at wileyonlinelibrary.com]

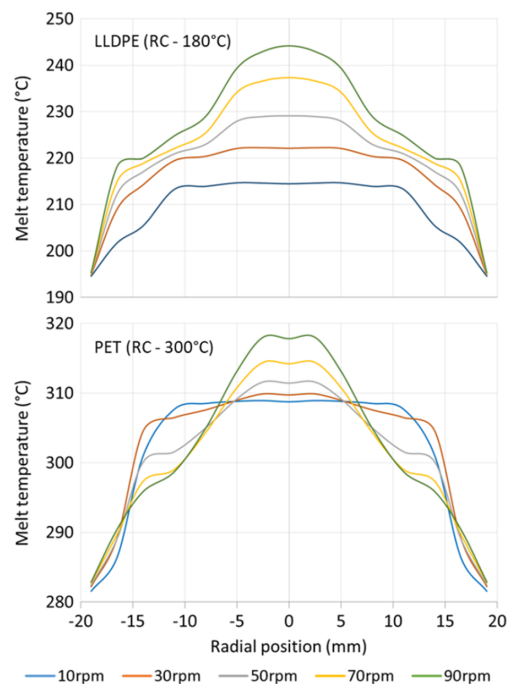


FIGURE 22 Melt temperature profiles for LLDPE and PET at the medium set temperature condition (B) with the rapid compression screw [Color figure can be viewed at wileyonlinelibrary.com]

(above 30 rpm), the melt temperature profile increases only at the middle of the flow (roughly across ± 9 mm from the centre of the flow) with the BF screw showing better melting performance compared to the GC screw. Such behavior might be due to the unique design of the BF screw to improve the melting/mixing process. This statement is supported by the previous studies^[8,32,42] who explained that the Maddox mixer at the end of the BF screw increases the thermal homogeneity of the melt. However, at higher screw speeds, melt temperature profiles across the melt flow gradually gain a W-shape forming a low temperature shoulder region a few millimetres (6–8 mm) away from the die wall. Kelly et al^[32] describe the W-shaped melt temperature profiles with the single-flight screws as a combination of rapid melting processes in the centre and the borders and a late melting of the solid bed in the middle of both. The higher temperatures at the centre of the melt flow and around the barrel wall are produced by a combination of the thermal energy transmitted by the metal and the mechanical energy generated by the viscous dissipation.^[5,11,45]

3.7.2 | Effects of the polymer type

Melt temperature profiles of LLDPE and PET at the set temperature condition B (medium) with the GC screw

are shown in Figure 22. The magnitudes of the melt temperature variations (particularly at the centre of the melt flow) are becoming greater as the screw speed increases for LLDPE ($\approx 0\text{--}45$ °C) than PET ($\approx 0\text{--}37$ °C). However, PET profiles at higher screw speeds present an A-shape. This pattern implies that the temperature of the melt close to the centre of the flow increases quite rapidly than the melt close to the die wall. An extrusion process is a combination of mechanical and thermal interactions, with some possible chemical reactions involved at high temperatures.^[40] Moreover, the nature of how polymers undergo with these operations will determine the thermal stability/quality of the melts.^[40] Various studies^[68–70] have been made to analyze the thermal stability of polymers and found that it is highly dependent upon the intrinsic properties of the materials. LLDPE is a flexible linear polymer with a very low degree of short uniform branches. Furthermore, PET is a strong and stiff polymer with a large aromatic ring in its chain structure.^[39] These statements suggest that the flexible backbone of the LLDPE is more capable in withstanding higher shear rates than the PET with a rigid chain. Also, the levels of the thermal and mechanical interactions are determined by the variations of the melt viscosity. However, the melt viscosity is a parameter that cannot be directly monitored and hence the melt pressure and temperature are commonly used to monitor the process quality and

functionality in current industrial practice. Consequently, the thermal stability should be studied with reference to the molecular weight, MWD, and the capacity of the material to overcome the possible mechanical stresses.^[40]

3.7.3 | Effects of the barrel/die set temperature

Temperature profiles of PS across the melt flow at set temperature conditions A (low) and C (high) with the GC screw are shown in Figure 23. Moreover, a polychromatic representation of the graphs shown in Figure 23 is given in Figure 24 and this provide a clear comparison of the melt temperature behaviour across the melt flow at low and high set temperature conditions.

As evident from these figures, the melt temperature distribution across the melt flow is dependent upon the barrel set temperature where the “A” shaped profile at the low set temperature condition has changed to a “W” shape particularly at high speeds with the high set temperature condition. Hence, the appropriate selection of the barrel/die set temperatures is crucial in achieving the best possible met thermal quality and also for the optimum use of energy during the process operation.

3.8 | Shear viscosity

The shear viscosity of LDPE, PS, and PMMA were obtained from steady shear tests and the results obtained are shown in Figure 25. The non-Newtonian behavior of a polymer (stress and shear rate relationship) is described by the power law model given in Equation (2).

$$\tau = K\dot{\gamma}^n \tag{2}$$

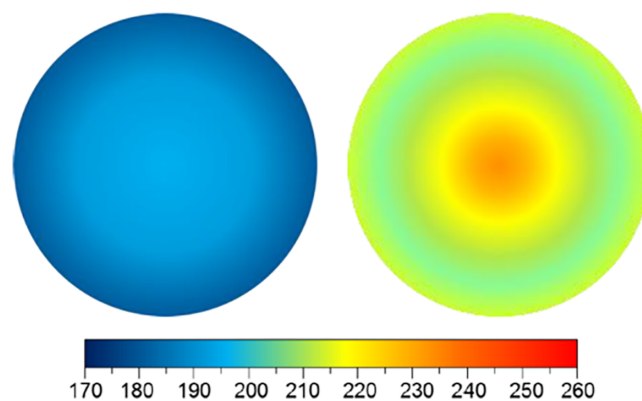


FIGURE 24 A polychromatic representation of the melt temperature distribution across the melt flow for PS processed at low (left) and high (right) barrel set temperature with the rapid compression screw [Color figure can be viewed at wileyonlinelibrary.com]

Where τ is the shear stress, K is the flow consistency index, $\dot{\gamma}$ is the shear rate and n is the power law index. The Carreau model^[71] describes the shear rate dependence of the viscosity over a wide range of shear rates (eg, this might be useful at very high and very low shear rates where power law may not be applicable). Moreover, Williams-Landel-Ferry (WLF) equation^[72] represents the temperature dependence of viscosity for amorphous polymer melts. For all the polymers used in this study, the viscosity decreases with the increase of both the shear rate and the temperature. Dealy^[73] and Abeykoon et al^[8] have analyzed the tendency of modelled curves with experimental curves for LDPE and PS at different temperatures and shear rates, and the results achieved in this study are in agreement those previous works.

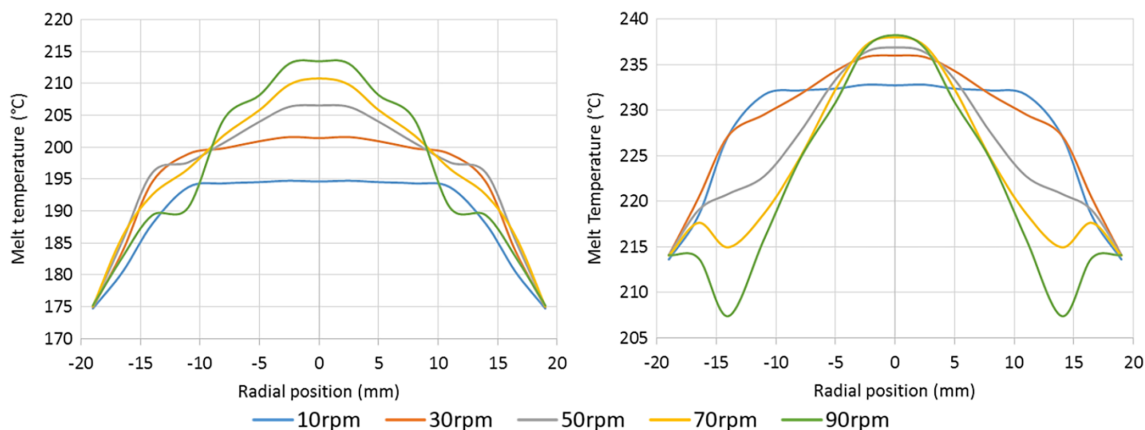


FIGURE 23 Melt temperature profiles for PS processed at low (left) and high (right) barrel set temperature with the rapid compression screw [Color figure can be viewed at wileyonlinelibrary.com]

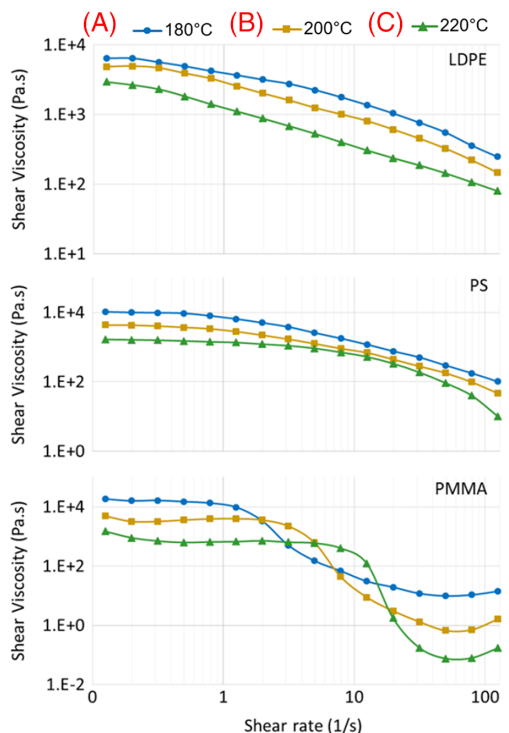


FIGURE 25 The shear viscosity of LDPE, PS and PMMA at low (A), medium (B), and high (C) set temperatures [Color figure can be viewed at wileyonlinelibrary.com]

The shear viscosity of PMMA shows a slight drop at a shear rate of around 2 s^{-1} and this continues up to 50 s^{-1} and starts to rise again despite the temperature. Vallés et al^[74] reported similar results for a virgin PMMA and also for a graphene based PMMA nano-composite. Such behavior reported with PMMA might be attributed to the collision between chain entanglements at very high shear rates regardless the temperature.^[75]

In another context, the results can be analyzed according to the melt-volume flow rate (MVR) of the materials. It was expected that for PMMA with a MVR of $3 \text{ cm}^3/10 \text{ minutes}$, the viscosity will be higher than that of PS with a MVR of $12 \text{ cm}^3/10 \text{ minutes}$. This negative correlation represents a decrease in the viscosity when the material can flow easily. However, the MVR do not predict any unusual behaviors or the exact share rates that they would occur.

3.9 | Viscoelastic modulus

The effects of temperature on linear viscoelastic curves for PMMA are presented in Figure 26. The most interesting aspect of the curves is that the crossover point takes place at a higher angular velocity as temperature increases. The storage modulus G' represents the elastic

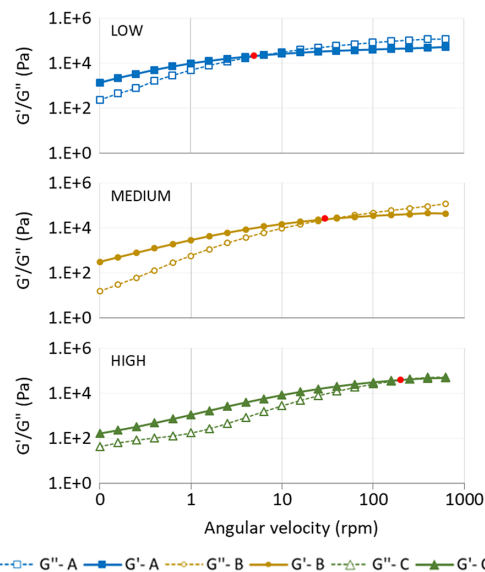


FIGURE 26 Storage (G') and loss (G'') moduli for PMMA at low, medium and high set temperatures [Color figure can be viewed at wileyonlinelibrary.com]

part of a material and the loss modulus G'' is related to the viscous region.^[38,41,63,76] Moreover, the crossover point indicates that the mechanical energy exceeds the intermolecular forces and the material starts to flow.^[77] Hence, it is possible to assume that the level of elasticity of PMMA increases as the temperature increases.^[78] The analysis of these types of properties of materials might help to improve the selection of the most appropriate processing conditions for extrusion processes.

3.10 | Rheological and physical instabilities

The processed raw polymer samples of LDPE, PS, and PMMA are shown in Figure 27 and samples are labeled as minimum (MIN), intermediate (INT) and extreme (EXT) conditions as was explained in Table 5. From these samples, three melt instabilities can be distinguished. First, at intermediate and extreme conditions, the extrudates present melt fracture with distorted shapes and smooth surfaces.^[79] The main reason for melt fracture would be the level of pressure in the die land.^[64] However, this depends on the material properties as well.^[81] Of the three materials, PMMA is the polymer which exhibits a several grades of melt fracture. As was reported in the previous studies^[80], PMMA showed spiral-helical type of distortions, and this may be attributed to the high viscosity of the material and hence its high resistance to flow.

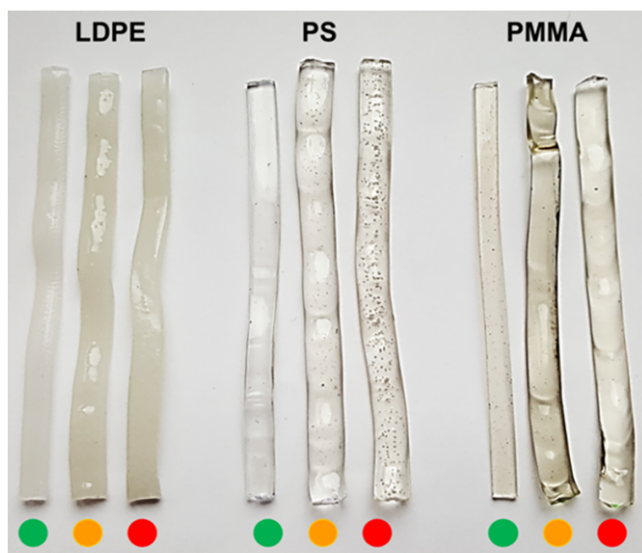


FIGURE 27 Polymer extrudates: at MIN (green), INT (orange), and EXT (red) conditions [Color figure can be viewed at wileyonlinelibrary.com]

Second, the extrudates start to swell at intermediate conditions. PS-INT is the sample which exhibits the greatest swelled appearance and it is caused by the tension applied to the melt when it is forced to flow through the die.^[20] The polymer chains are usually oriented in the direction of the flow when they are in the die. After this, in the die land area, they relax and the reentanglement of chains occurs due the elastic portion of the material.^[79] Swelling might occur if the die residence time is shorter than that of the material relaxation time^[20] that is, the die of the MiniLab TSE should be longer to avoid this behavior.

Thirdly, the presence of bubbles due to the presence of water at high temperatures and screw speeds.^[81] As shown in Figure 27, air bubbles are clearly visible of the PS sample. The water absorption of the grade of PS used in this work is less than 0.1%. This might be due to the remnant solids mixed with the melt and the normal air expelling process turns difficult at such high temperatures and speeds.^[20] Hence, it might be good to predry this type of low hygroscopic materials to avoid the possible bubble formation.

Moreover, the nature of the surface of each raw polymer sample before and after the shaping is detailed in Figure 28. Some kind of wavy surfaces are presented by PS-MIN and PMMA-EXT which might be due to the melt fracture conditions. However, the striation exhibited by LDPE-MIN surface might be a melt distortion known as sharkskin. It is known that, polyolefins, polymers with a high molecular weight and a narrow MWD are prone to sharkskin and usually it is not visible to naked eye.^[14,80]

	Original surface	Shaped surface	Observations
LDPE-MIN			Appearance: Waxy Colour: Translucent Surface: Grooved Diagonal discontinuities and longitudinal striation. The thickness of grooves varies between 90 – 750 μm .
LDPE-INT			Appearance: Waxy Colour: Translucent Surface: Slightly bubbled Light content of bubbles. Surface with a 91% polymer, 8% superficial bubbles and 1% background bubbles. Bubbles sizes are between 200 - 500 μm .
LDPE-EXT			Appearance: Waxy Colour: Translucent Surface: Highly bubbled High content of bubbles. Surface with 85% polymer, 14% superficial bubbles and 1% background bubbles. Bubbles sizes are between 200 - 600 μm .
PS-MIN			Appearance: Glassy Colour: Transparent Surface: Slightly wavy Dense content of short waves. Wave separation is around 1100 μm .
PS-INT			Appearance: Glassy Colour: Transparent Surface: Slightly bubbled Very light content of bubbles. Surface with 97.5% polymer, 1% bubbles and 1.5% bubbles conglomeration. Bubbles sizes are around 100 μm .
PS-EXT			Appearance: glassy Colour: transparent Surface: highly bubbled Very high content of bubbles. Surface with 83% polymer, 7% bubbles and 10% bubbles conglomeration. Bubbles sizes are around 300 μm .
PMMA-MIN			Appearance: glassy Colour: transparent Surface: smooth Completely smooth and homogeneous, no presence of bubbles, nor of waves. The shaped surface is emphasising the existence of light reflection.
PMMA-INT			Appearance: glassy Colour: transparent Surface: smooth Smooth surface with minimal presence of bubbles (0.4%).
PMMA-EXT			Appearance: glassy Colour: transparent Surface: highly wavy Dense content of large waves. Wave separation is irregular. It varies between 1000 - 2000 μm .

FIGURE 28 Surface characteristics of extrudates [Color figure can be viewed at wileyonlinelibrary.com]

Moreover, the melt rupture can be occurred in the die exit due to the possible low temperature conditions.^[14]

3.11 | Analysis of correlations between parameters

An attempt was made to study the possible correlations between the parameters studied. A summary of non-scaled trend lines of different processing parameters

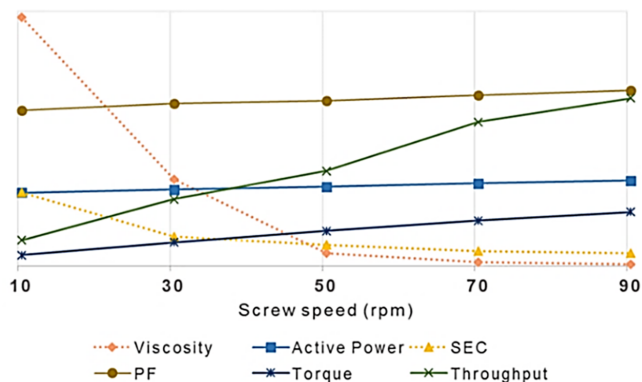


FIGURE 29 Trend lines of the different parameters in the extrusion process [Color figure can be viewed at wileyonlinelibrary.com]

(viscosity, active power, extruder SEC, PF, torque, and mass throughput) are presented in Figure 29. It can be noticed that the viscosity and the SEC tend to decrease while PF, throughput, AP, and torque tend to increase with the screw speed. Also, it can be claimed that the shear and viscous heat generations increase with the screw speed and this heat contributes in decreasing the viscosity. Moreover, the drive motor can become more energy efficient at high speeds and also the process output increases with the speed, hence the SEC should go down with these changes.

Table 6 shows the Pearson correlation coefficient and the the parentage of R^2 between these parameters measured when processing of PMMA with the MiniLab TSE at 210 °C. The correlation is perfect (inverse or direct) when the absolute value is the ± 1 and it is weaker as the value becomes closer to zero. Additionally, it is important to mention that a correlation does not imply that changes in one parameter can cause changes in the other (Table 6).^[82]

Moreover the parentage of R^2 (the determination coefficient) represents the degree of reliability of the applied statistical model to the predict future values.^[83] Mainly, three types of correlations can be distinguished:

- The viscosity has an indirect correlation with the mass throughput, torque, AP and PF. Moreover, the low values of R^2 imply that the Pearson model is not reliable to predict this behavior. Hence, a nonlinear model should be applied to achieve a reliable and an accurate model.
- The viscosity has a linear relationship with the SEC. However, the reliability needs to be improved.
- The Pearson coefficients between the mass throughput, torque, AP and PF show direct linear correlations with high values of R^2 . Hence, linear models should be able to predict their behavior with good accuracy.

TABLE 6 Pearson correlation coefficients for various processing parameters

	1.	2.	3.	4.	5.	PF
1. Viscosity	-	.84	-.49	-.52	-.47	-.55
		72%	24%	28%	22%	31%
2. SEC		-	-.87	-.88	-.85	-.89
			76%	79%	73%	79%
3. Throughput			-	.99	.99	.99
				99%	99%	98%
4. Torque				-	.99	.99
					99%	98%
5. Active power					-	.99
						98%

The simple Pearson correlation suggested a liner correlation between the mass throughput, torque, AP and PF. However, these data should be analyzed for possible cross-correlations between them. Such correlations should help in predicting/understanding the state-of-the-art of the processing behavior offering multiple benefits to the polymer processing industry.

4 | CONCLUSIONS

In general, it can be concluded that materials' rheology has a vital effect on the energy consumption in polymer extrusion in agreement with the previous investigations as well. The SEC for both single and twin screw extruders tends to decrease with the increasing screw speed. In order to increase the rate of production, it can be recommended to work with the maximum possible processing speed, provided that it does not compromise the thermal stability (ie, melt quality) of the molten material. AP, mass throughput, torque, and PF tend to increase with the screw speed. However, the magnitude of the increment will depend on the barrel/die set temperature in conjunction with the viscoelastic properties of each material. With the twin screw extruder, PMMA presented the highest values of SEC. Similarly, the greatest viscosities were reported for the same material, suggesting a possible correlation between these two parameters. Polymer melt rheology shows some links with the fluctuations in the melt temperature, torque, PF, and AP. High viscosities tend to increase the magnitude of the fluctuations. Since the viscosity decreases with the set temperature, high temperatures would be recommended. However, this action compromises the thermal efficiency. The onset shear rate for PMMA showed to increase with the set temperature. Therefore, this

parameter should be taken into account for appropriate selection of the screw speed. The linear tendency of decreasing of mass throughput, torque, AP, and PF can be analyzed by advanced statistical techniques to explore possible cross-correlations between these variables, due to the positive results that they reported with the Pearson single correlation. Additionally, regarding the electrical analysis of the MiniLab TSE, the data obtained as well as the quality of the extrudates produced are reliable. However, the functional components of this machine, due to its smaller size, are not suitable to be compared with an industrial scale extruder such as the medium scale SSE used in this work.

5 | RECOMMENDATIONS FOR FUTURE WORK

The melt viscosity of polymers should be analyzed including the use of additives, plasticisers, fillers, lubricants, stabilisers, colourants, and other solutions popular within the industrial extrusion processes. Such materials may completely change the rheological behavior as well as the SEC during processing. In this study, the effects of the screw geometry were tested. The type of die should also be tested. It will allow measuring the variations of the melt pressure with each different design. The stress relaxation should also be analyzed on the swelling ratio of a material for different temperatures. This should help in the selection of the correct screw speed. The gap between the plates in the parallel-plate rheometer should be modified in the range of 5 μm to 1 mm. This variation in the gap may allow analyzing the shear homogeneity widely in the melt and also how it can be applied in the extrusion processes.

REFERENCES

- [1] EURecipe. Low energy plastic processing. *European Best Practice Guide*, <https://ec.europa.eu/energy/intelligent/projects/en/projects/recipe> (2006).
- [2] C. Abeykoon, A. L. Kelly, E. C. Brown, J. Vera-Sorroche, P. D. Coates, E. Harkin-Jones, K. B. Howell, J. Deng, K. Li, M. Price, *Appl. Energy* **2014**, *136*, 726.
- [3] J. Deng, K. Li, E. Harkin-Jones, M. Price, M. Fei, A. Kelly, J. Vera-Sorroche, P. Coates, E. Brown, *Trans. Inst. Meas. Control* **2014**, *36*, 382.
- [4] J. Deng, K. Li, E. Harkin-Jones, M. Price, N. Karnachi, A. Kelly, J. Vera-Sorroche, P. Coates, E. Brown, M. Fei, *Appl. Energy* **2014**, *113*, 1775.
- [5] K. Kohlgrüber, *Co-Rotating Twin-Screw Extruders: Fundamentals, Technology, and Applications*, Carl Hanser Publishers, USA, **2008**.
- [6] Kruder, G. A. & Nunn, R. E. Optimizing energy utilization in extrusion processing. *SPE ANTEC Tech. Pap.* **1981**, pp. 648–652.
- [7] J. Vera-Sorroche, A. Kelly, E. Brown, P. Coates, N. Karnachi, E. Harkin-Jones, K. Li, J. Deng, *Appl. Therm. Eng.* **2013**, *53*, 405.
- [8] C. Abeykoon, A. L. Kelly, J. Vera-Sorroche, E. C. Brown, P. D. Coates, J. Deng, K. Li, E. Harkin-Jones, M. Price, *Appl. Energy* **2014**, *135*, 560.
- [9] C. Abeykoon, A. L. Kelly, J. Vera-Sorroche, E. C. Brown, P. D. Coates, J. Deng, K. Li, N. Karnachi, E. Harkin-Jones, M. Price, in *Int. Conf. Polym. Process. Soc. (PPS 29)*, Paper No: 486, Nuremberg, Germany, July 15–19, **2013**.
- [10] C. Abeykoon, K. Li, P. Martin, A. Kelly, *Int. J. Syst. Control Inf. Process.* **2012**, *1*, 71.
- [11] J. Deng, K. Li, E. Harkin-Jones, M. Price, *Commun. Comp. Inform. Sci.* **2013**, *355*, 533.
- [12] C. Abeykoon, A. L. Kelly, E. C. Brown, P. D. Coates, *Appl. Energy* **2016**, *180*, 880.
- [13] C. Abeykoon, M. McAfee, S. Thompson, K. Li, A. L. Kelly, E. C. Brown, in *PPS Europe/Africa Reg. M*, Paper Number: 22-O, Larnaca, Cyprus, October 18–21 **2009**.
- [14] Kelly A., *PhD Thesis*, University of Bradford, **1997**.
- [15] InterTradeIreland, A competitiveness analysis of the polymer and plastic industry on the island of Ireland, <http://www.intertradeireland.com/media/intertradeirelandcom/researchandstatistics/publications/tradeandbusinessdevelopment/CompetitiveAnalysisofthePolymer&PlasticsIndustryontheislandofIreland.pdf> **2018**.
- [16] British plastics federation, about the British plastics industry, <http://www.bpf.co.uk/Industry/Default.aspx> **2017**.
- [17] PlasticsEurope, https://www.plasticseurope.org/download_file/force/1568/181 **2018**.
- [18] R. Kent, *Rubb. Comp.* **2008**, *37*(2–4), 96.
- [19] J. Agassant, *Polymer Processing*, Hanser Publishers, Munich **1991**.
- [20] Wilkinson, A. N. & Ryan, A. J. *Polymer Processing and Structure Development*, Kulwer Academic Publishers, Dordrecht, Netherlands **1998**.
- [21] C. Rauwendaal, *Polymer extrusion*, 5th ed., Hanser Publishers, Munich **2014**.
- [22] Severs, E. T. *Rheology of Polymers*, Van Nostrand Reinhold Inc., USA **1962**.
- [23] R. O. Ebewele, *Polymer Science and Technology*, CRC Press, New York **2000**.
- [24] T. Osswald, J. Hernandez-Ortiz, *Polymer Processing*, Haaser Publishers, Munich **2006**.
- [25] Myers J., Advancements in screw design technology for the blown film industry, Barr Inc., www.tappi.org/content/enewsletters/eplace/2006/06PLA28.pdf **2018**.
- [26] Z. Tadmor, *Polym. Eng. Sci.* **1966**, *6*(3), 185.
- [27] Z. Tadmor, I. Klein, *Rubb. Chem. Technol.* **1969**, *42*(3), 780.
- [28] Z. Tadmor, C. G. Gogos, Principles of Polymer Processing (Google eBook). in *Handbook of Polymer Synthesis, Characterization, and Processing*, Wiley, New Jersey **2006**. <https://doi.org/10.1002/9781118480793.ch23>.
- [29] T. L. Vigo, L. J. Nowacki, *Energy Conservation in Textile and Polymer Processing*, American Chemical Society, Washington **1979**.
- [30] Abeykoon, C. & Kelly, A., in *13th Eur. Control Conf. (ECC 2014)*, Strasbourg, France, June 24–27 **2014**, pp. 1030–1035.

- [31] J. Vera-Sorroche, A. L. Kelly, E. C. Brown, T. Gough, C. Abeykoon, P. D. Coates, J. Deng, K. Li, E. Harkin-Jones, M. Price, *Chem. Eng. Res. Des.* **2014**, *92*, 2404.
- [32] A. L. Kelly, E. G. Brown, P. D. Coates, *Polym. Eng. Sci.* **2006**, *46*, 1706.
- [33] C. Abeykoon, M. McAfee, K. Li, P. J. Martin, J. Deng, A. L. Kelly, in *IEEE LSMS/ICSEE2010 International Conference 2010*, (Part II, LNCS 6329), Wuxi, China **2010**, pp. 9–20.
- [34] E. Lai, D. W. Yu, *Polym. Eng. Sci.* **2000**, *40*(5), 1074.
- [35] R. S. Mallouk, J. M. McKelvey, *Ind. Eng. Chem.* **1953**, *45*, 987.
- [36] K. J. Wilczyński, *Polym. Technol. Eng.* **1996**, *35*(3), 449.
- [37] C. D. Han, *Rheology in Polymer Processing*, Academic Press Inc., Salt Lake City **1976**.
- [38] T. Osswald, N. Rudolph, *Polymer Rheology: Fundamentals and Applications*, Hanser Publications, Munich **2014**.
- [39] R. Young, P. Lovell, *Introduction to Polymers*, CRC Press, Florida **2011**.
- [40] Rauwendaal C., *Polymer Mixing: A Self-study Guide*, Hanser, Munich **1998**. <https://doi.org/10.1016/B978-1-56990-516-6.50001-0>
- [41] Dealy, J. M., Wissburn K. F. *Melt Rheology and Its Role in Plastics Processing*, Kluwer Academic Publishers, Dordrecht, **1990**.
- [42] E. C. Brown, A. L. Kelly, P. D. Coates, *Rev. Sci. Instrum.* **2004**, *75*, 4742.
- [43] C. Abeykoon, M. McAfee, K. Li, P. J. Martin, A. L. Kelly, *J. Mater. Process. Technol.* **2011**, *211*, 1907.
- [44] C. Abeykoon, *Polymer Extrusion: A Study on Thermal Monitoring Techniques and Melting Issues*, Lamber Academic Publishing, Saarbrücken **2012**.
- [45] J. Vera-Sorroche, A. L. Kelly, E. C. Brown, P. D. Coates, *Polym. Eng. Sci.* **2015**, *55*, 1059.
- [46] C. Abeykoon, *Modelling and Control of Melt Temperature in Polymer Extrusion*, Queen's University Belfast, Belfast, UK **2011**.
- [47] C. Abeykoon, *Control Eng. Pract.* **2016**, *51*, 69.
- [48] C. Abeykoon, *IEEE Trans. Ind. Electron.* **2014**, *61*(12), 7113.
- [49] C. Abeykoon, *IEEE Trans. Fuzzy Syst.* **2014**, *22*(6), 1413.
- [50] C. Abeykoon, P. J. Martin, A. L. Kelley, K. Li, E. C. Brown, P. D. Coates, *Polym. Eng. Sci.* **2014**, *54*(10), 2430.
- [51] C. Abeykoon, P. J. Martin, A. L. Kelly, E. C. Brown, *Sensors Actuators A: Phys.* **2012**, *182*, 16.
- [52] C. Abeykoon, K. Li, M. McAfee, P. J. Martin, Q. Niu, A. L. Kelly, J. Deng, *Control Eng. Pract.* **2011**, *19*(8), 862.
- [53] P. Plochocki, S. K. Dey, K. Wilczynski, *Polym. Eng. Sci.* **1986**, *26*(14), 1007.
- [54] K. Wilczynski, *Polymer-Plastic Technol. Eng.* **1989**, *28* (7–8), 671.
- [55] A. Nastaj, K. Wilczynski, *Polymers* **2020**, *12*(1), 149.
- [56] J. A. Covas, O. S. Carneiro, P. Costas, A. V. Machado, J. M. Maia, *Plast. Rubb. Comp.* **2004**, *33*(1), 55.
- [57] A. G. Cunha, J. A. Covas, P. Oliveira, *IMA J. Manag. Mathemat.* **1998**, *9*(3), 267.
- [58] J. A. Covas, A. G. Cunha, P. Oliveira, *Polym. Eng. Sci.* **1999**, *39* (3), 443.
- [59] J. A. Covas, A. Gaspar-Cunha, *Plast. Rubb. Comp.* **2004**, *33* (9–10), 416.
- [60] C. Wang, J. Wang, C. Yu, B. Wu, Y. Wang, W. Li, *Polym. Testing* **2014**, *33*, 138.
- [61] M. Yousfi, S. Alix, M. Lebeau, J. Soulestin, M. Lacrampe, P. Krawczak, *Polym. Test.* **2014**, *40*, 207.
- [62] Y.-F. Mei, B.-H. Guo, J. Xu, *Chinese Chem. Lett.* **2016**, *27*, 588.
- [63] A. L. Kelly, T. Gough, B. R. Whiteside, P. D. Coates, *J. Appl. Polym. Sci.* **2009**, *114*, 864.
- [64] M. Kontopoulou, *Applied Polymer Rheology: Polymeric Fluids with Industrial Applications*, Wiley, New Jersey **2011**.
- [65] Cantor, K. M. Analyzing extruder energy consumption, *SPE ANTEC Tech. Papers*, **2010**, pp. 603–609.
- [66] A. Franck, *TA Instr.* **2004**, *118*, 1.
- [67] A. Kumar, D. D. Jones, G. E. Meyer, M. A. Hanna, *J. Food Process Eng.* **2015**, *38*, 125.
- [68] T. R. Rompton, *Thermal Stability of Polymer*, Smithers Rapra Publishing, Shrewsbury **2012**.
- [69] R. E. Florin, L. A. Wall, D. W. Brown, L. A. Hymo, J. D. Michaelsen, *J. Res. Natl. Bur. Stand. (1934)* **1954**, *53*(2), 121.
- [70] S. A. Jabarin, E. A. Lofgren, *Polym. Eng. Sci.* **1984**, *24*, 1056.
- [71] P. J. Carreau, *Trans. Soc. Rheol.* **1972**, *16*(1), 99.
- [72] J. D. Ferry, R. F. Landel, M. L. Williams, *J. Appl. Phys.* **1995**, *26*(4), 359.
- [73] J. M. Dealy, J. Wang, *Melt Rheology and Its Applications in the Plastics Industry*, Springer, Munich **2013**. <https://doi.org/10.1007/978-94-007-6395-1>.
- [74] C. Vallés, A. M. Abdelkader, R. J. Young, I. A. Kinloch, *Compos. Sci. Technol.* **2015**, *111*, 17.
- [75] Ceramic Processing E-zine. Dingerceramics.com, **2006**.
- [76] A. Franck, *TA Instr.* New Castle, DE, USA AN004 **2004**.
- [77] A. S. Merenga, G. A. Katana, *Int. J. Polym. Mater.* **2010**, *60*, 115.
- [78] R. R. Rahalkar, *Rheol. Acta* **1989**, *28*, 166.
- [79] J. R. Wagner, E. M. Mount, H. F. Giles, *Extrusion: The Definitive Processing Guide and Handbook*, 1st ed., William Andrew Inc., Norwich, USA **2014**. <https://doi.org/10.1016/B978-1-4377-3481-2.00001-6>.
- [80] C. Stamboulides, S. G. Hatzikiriakos, *Int. Polym. Process.* **2006**, *21*, 155.
- [81] Wojewodka, R. Lubrizol & Marruchella, D. Emerson, P. M.. Online analytics improves batch operations. *Chem. Process.*, **2011**.
- [82] G. W. Heiman, *Basic Statistics for the Behavioral Sciences*, Wadsworth/Cengage Learning, Belmont, USA **2011**.
- [83] Martínez Rodríguez, E. *Errores frecuentes en la interpretación del coeficiente de determinación lineal*. Anu. Jurídico y Económico Eскур., **2005**.

How to cite this article: Abeykoon C, Pérez P, Kelly AL. The effect of materials' rheology on process energy consumption and melt thermal quality in polymer extrusion. *Polym Eng Sci.* 2020; 60:1244–1265. <https://doi.org/10.1002/pen.25377>